Scalable Nitrogen-Enriched Porous Sub-100 nm Graphitic Carbon Nanocapsules for Efficient Oxygen Reduction Reaction in Different Media†

Kamel Eid[a*], Ali A. Abdelhafiz[b*], Safwat Abdel-Azeim[c], Rajender S. Varma[d], and Mohamed F. Shibl[e]

a. *Gas Processing Center (GPC), College of Engineering, Qatar University, Doha 2713, Qatar. *E-mail:* kamel.eid@qu.edu.qa

b. *Department of Nuclear Science Engineering, Massachusetts Institute of Technology, Cambridge, MA 02139, USA. *E-mail: ali_m@mit.edu*

c. *Center for Integrative Petroleum Research (CIPR), College of Petroleum Engineering and Geosciences, King Fahd University of Petroleum and Minerals (KFUPM), Dhahran 31261, Saudi Arabia*

d. *Regional Centre of Advanced Technologies and Materials, Czech Advanced Technology and Research Institute, Palacky University, Slechtitelu 27, 783 71 Olomouc, Czech Republic.*

e. *Renewable Energy Program, Center for Sustainable Development, College of Arts and Sciences, Qatar University, Doha 2713, Qatar*

Experimental and Equipment

Chemicals

Melamine (($C_3H_6N_6$) 99.0 %), tetraethylorthosilicate (TEOS), resorcinol, formaldehyde, ethanol (98%), ammonium hydroxide (NH_4OH (25 %), and potassium hydroxide (KOH), ≥ 85 % powder) were purchased from Sigma-Aldrich (Munich, Germany). Commercial Pt/C catalyst E-TEK Pt/C (20 wt % Pt nanoparticles 2-5 nm on Vulcan XC-72R carbon support) was procured from Alfa Aesar.

Synthesis of N-HMPC

N-HMPC nanocapsules are prepared by mixing Pluronic F127 (0.13 g), (20.4 mmol) of NH_4OH with 50 mL ethanol/water mixture under vigorous stirring for 30 min at 35 °C before subsequent addition of TEOS (6.4 mmol), melamine (0.8 g), resorcinol (0.2 g), and formaldehyde solution (3.6 mmol), respectively under stirring for 5 h at 50 °C, followed by refluxing at 100 °C for 24 h. Then, the mixture is centrifuged at 10,000 rpm and washed with ethanol/water (3/1) for 3 times before drying at 100 °C for 4 h and annealing in a tube furnace at 900 °C for 2h (3 °C/min) under nitrogen. After cooling to room temperature, the obtained powder was immersed in KOH solution (10 wt %) in hot water (80 °C) for 20 h to leach out the silica core.

The same approach is used to prepare nitrogen-free porous carbon (HMPC) but in the absence of melamine and with fixing all other conditions and parameters.

Materials Characterization

The structure of the as-formed materials is analyzed by a transmission electron microscopy (TEM) (TecnaiG220, FEI, USA) equipped with a Gatan CCD794 camera, high-resolution TEM (HRTEM) and energy dispersive X-ray (EDX). The crystallinity is investigated by a wide-angle X-ray diffraction pattern (XRD) (X`Pert-Pro MPD diffractometer, PANalytical, Netherlands) with a Cu Kα X-ray source (λ = 1.540598 Å). The surface composition and electronic structures are investigated by an X-ray photoelectron spectroscopy (XPS) Kratos Axis Ultra XPS spectrometer equipped with a monochromatic Al Kα radiation source (1486.6 eV) under a UHV environment (ca. 5×10^{-9} Torr). The Nitrogen adsorption/desorption isotherms are investigated with a Quantachrome Autosorb 3.01 instrument. The Raman spectra were measured on a PerkinElmer RamanStation 400 spectrometer with a 785 nm laser as an excitation source.

Oxygen reduction reaction

The ORR was conducted using a CHI 832C electrochemical analyzer (Chenhua Co., Shanghai, China) using a three-electrode alkaline resistant cell including an Ag/AgCl (reference electrode), Pt wire (counter electrode), and rotating disk electrode ((RDE) working electrode). The RDE was coated with 5 µg of each catalyst, followed by addition of 5 µL Nafion (0.05 %) and fully dried before the measurements. Cyclic voltammograms (CVs) are initially measured in N_2-saturated 0.1 M KOH between 0.25 to -1.2 V for 50 cycles at 200 mV s^{-1} for removing any impurities from the RDE surface. The ORR polarization curves are measured on an RRDE-3A rotation system (ALS Co. Ltd, Japan) in an O_2-saturated 0.1 M KOH at a rotating speed of 1600 rpm, at a sweeping rate of 20 mV s^{-1} at room temperature. The Koutecky-Levich equation is used to calculate the kinetic current (j_k), which can be described as follow:
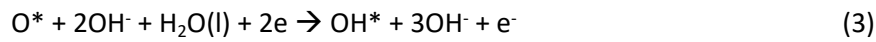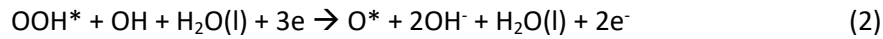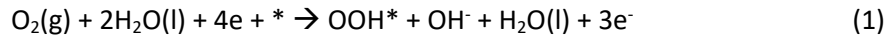
$$j_k = j \times j_d / j_d - j$$

where j is the measured current and j_d is the diffusion-limited current. All the measured currents are normalized to the geometric area of the working electrode, while the potentials are recorded after the IR-drop correction during the ORR.

DFT computational details

All Density functional theory (DFT) simulations were carried out using the Vienna ab initio simulation package (VASP) with the projector augmented wave pseudopotentials (PAW), and the periodic boundary conditions).[1-3] The Brillouin zone was sampled using 3×3×1 Monkhorst-pack gamma centered mesh, and Gaussian smearing of 0.02 eV was used for the occupations of the electronic levels. Perdew−Burke−Ernzerhof (PBE) functional within the generalized gradient approximation (GGA) was used to describe the electron interaction energy of exchange-correlation. The electronic energies were converged within the limit of 10^{-7} eV and the cutoff of 520 eV was used. All geometries were optimized using 0.01 eV/Å

force criteria. All the calculations were spin-polarized. In systems such as HMPC and N-HMPC Van Der Waals (vdW) dispersion corrections are important to accurately describe the geometries and energies of such systems. VDW corrections adopted Grimme's D2 scheme). [1-3] N-HMPC model is generated using 6 x 6 x 1 of HMPC sheet (72 atoms) with 25 at % of nitrogen, which corresponding to the experimental atomic ratio.

The ORR reaction diagram on the N-HMPC model calculated followed the well-established computational hydrogen electrode approach pioneered by Nørskov et al.[2] The details of our adopted approach is based on the one detailed.[1-3] In the alkaline media, the four-electron ORR steps are modelled as the following:

$$O_2(g) + 2H_2O(l) + 4e + * \rightarrow OOH^* + OH^- + H_2O(l) + 3e^- \tag{1}$$

$$OOH^* + OH + H_2O(l) + 3e \rightarrow O^* + 2OH^- + H_2O(l) + 2e^- \tag{2}$$

$$O^* + 2OH^- + H_2O(l) + 2e \rightarrow OH^* + 3OH^- + e^- \tag{3}$$

$$OH^* + 3OH^- + e \rightarrow 4OH + * \tag{4}$$

The free energies of all the species at an applied electrode potential U were calculated as follows: $G(U) = \Delta E + \Delta ZPE - T\Delta S - neU$, where n is the electron number of such state and ΔE represents the change in enthalpy, which is considered from the DFT total energies, ΔZPE represents the change in zero-point energy (Table S1) and ΔS represents the change in entropy. The adsorption free energies of ΔG_{OOH^*}, ΔG_{O^*}, and ΔG_{OH^*} are considered as the free energy of OOH, O, and OH radicals in the electrolyte solution.

Therefore, at the equilibrium potential U_0, the free energy change of four steps can be summarized as follow:

$$\Delta G_1 = G_{OOH^*} + G_{H2O(l)} - G_* - 3G_{OH^-} - 3eU \tag{5}$$

$$\Delta G_2 = G_{O^*} - G_{OOH^*} + G_{OH^-} - eU \tag{6}$$

$$\Delta G_3 = G_{OH^*} - G_{H2O(l)} - G_{O^*} + G_{OH^-} - eU \tag{7}$$

$$\Delta G_4 = - G_{OH^*} + G_* + G_{OH^-} + eU \tag{8}$$

In our calculations, the equilibrium potential U_0 for ORR was considered to be 0.455 V and 1.23 V *vs* NHE in alkaline and acidic media, where the reactant and product are at the same energy level. The free energy of $H_2O(l)$ is derived as $G_{H2O}(l) = G_{H2O}(g) + RT \times \ln(p/p0)$, where $G_{H2O(g)}$ obtained directly from DFT calculations, R is the ideal gas constant, T = 298.15K, $p = 0.035$ bar, and $p^0 = 1$ bar. The free energy of $O_2(g)$ has been considered as $G_{O2}(g) = 2G_{H2O}(l) - 2G_{H2} + 4.92$ eV. The free energy of OH^- derived as $G_{OH^-} = G_{H2O}(l) - G_{H+}$, where $G_{H+} = 1/2G_{H2} - k_BT \ln 10 \times pH$, and pH=13.

In the acidic media, the four-electron ORR elementary steps are:

$$O_2(g) + 4H^+ + 4e- + * \rightarrow OOH^* + 3H^+ + 3e^- \tag{9}$$

$$OOH^* + 3H^+ + 3e^- \rightarrow O^* + H_2O(l) + 2H^+ + 2e^- \tag{10}$$

O* + H₂O(*l*)   + 2H⁺ + 2e- → OH* + H₂O(*l*) + H⁺ + e⁻   (11)

OH* + H₂O(*l*) + H⁺ + e- → 2H₂O(*l*) + *   (12)
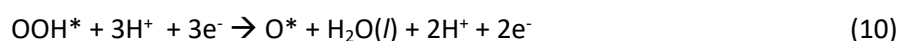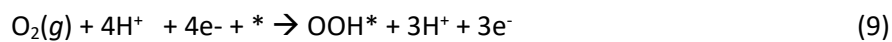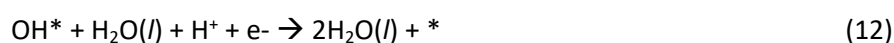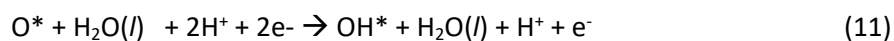
Similarly, as in the alkaline medium, the free energies of the elementary steps can be written as the following:

$$\Delta G_1 = G_{OOH*} - G_* + 3G_{H+} - G_{O2} - 2G_{H2} - 3eU \qquad (13)$$

$$\Delta G_2 = G_{O*} - G_{OOH*} + G_{H2O} - 3/2\ G_{H2} + 2G_{H+} - 2eU \qquad (14)$$

$$\Delta G_3 = G_{OH*} - G_{H2O(l)} - G_{O*} + G_{H+} - G_{H2} - eU \qquad (15)$$

$$\Delta G_4 = - G_{OH*} + G_* + G_{H2O} - 1/2\ G_{H2} + eU \qquad (16)$$

Table S1: Entropy and zero point energy for the adsorbed and gaseous phase states of molecules. The values for the adsorbed species are calculated using the finite difference method as implemented in VASP, while for the gaseous species are taken from ref.[3]

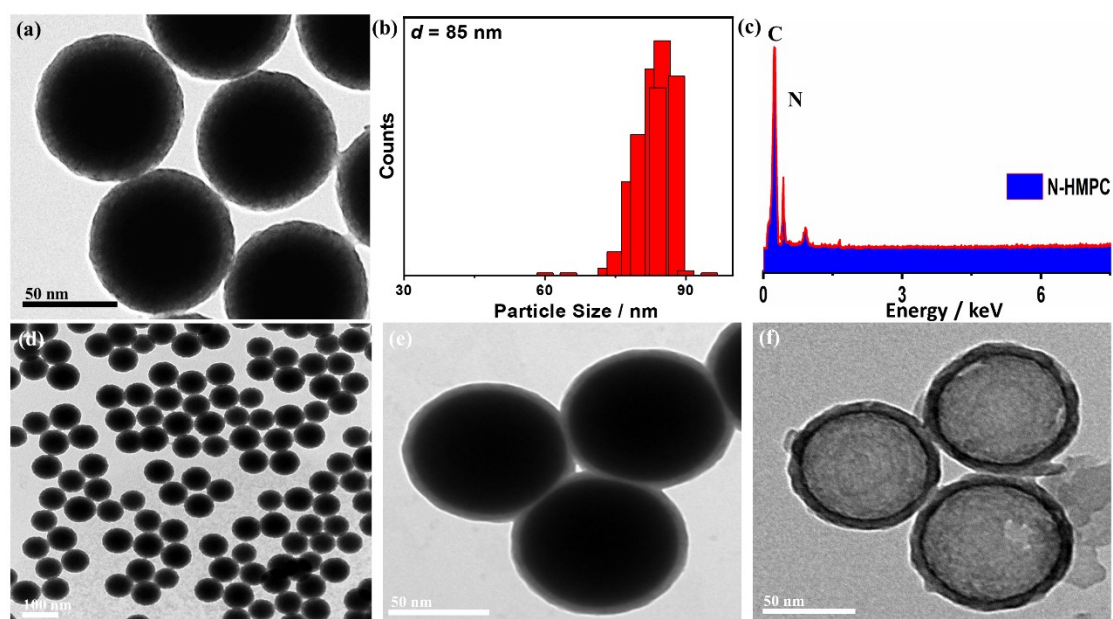|	ZPE	TS
H₂O	0.56	0.67
H₂	0.27	0.41
OH*	0.40	0.0
O*	0.10	0.0

Figure S1 (a) TEM image of N-HMPC before SiO₂ removal, (b) particle size distribution of N-HMPC and its EDX spectrum (c). (d) Low magnification TEM image and (e) high magnification TEM image of nitrogen-free HMPC before and (f) after colloidal SiO₂ removal.
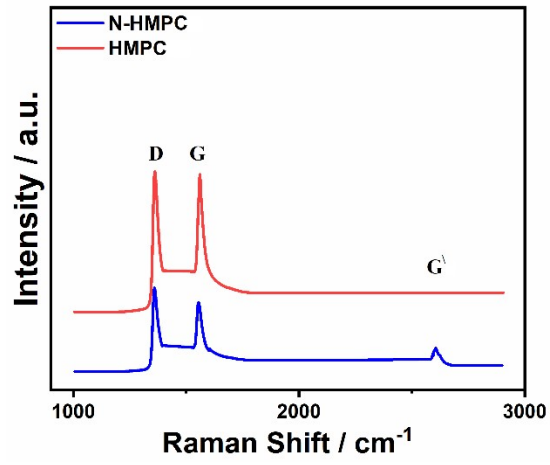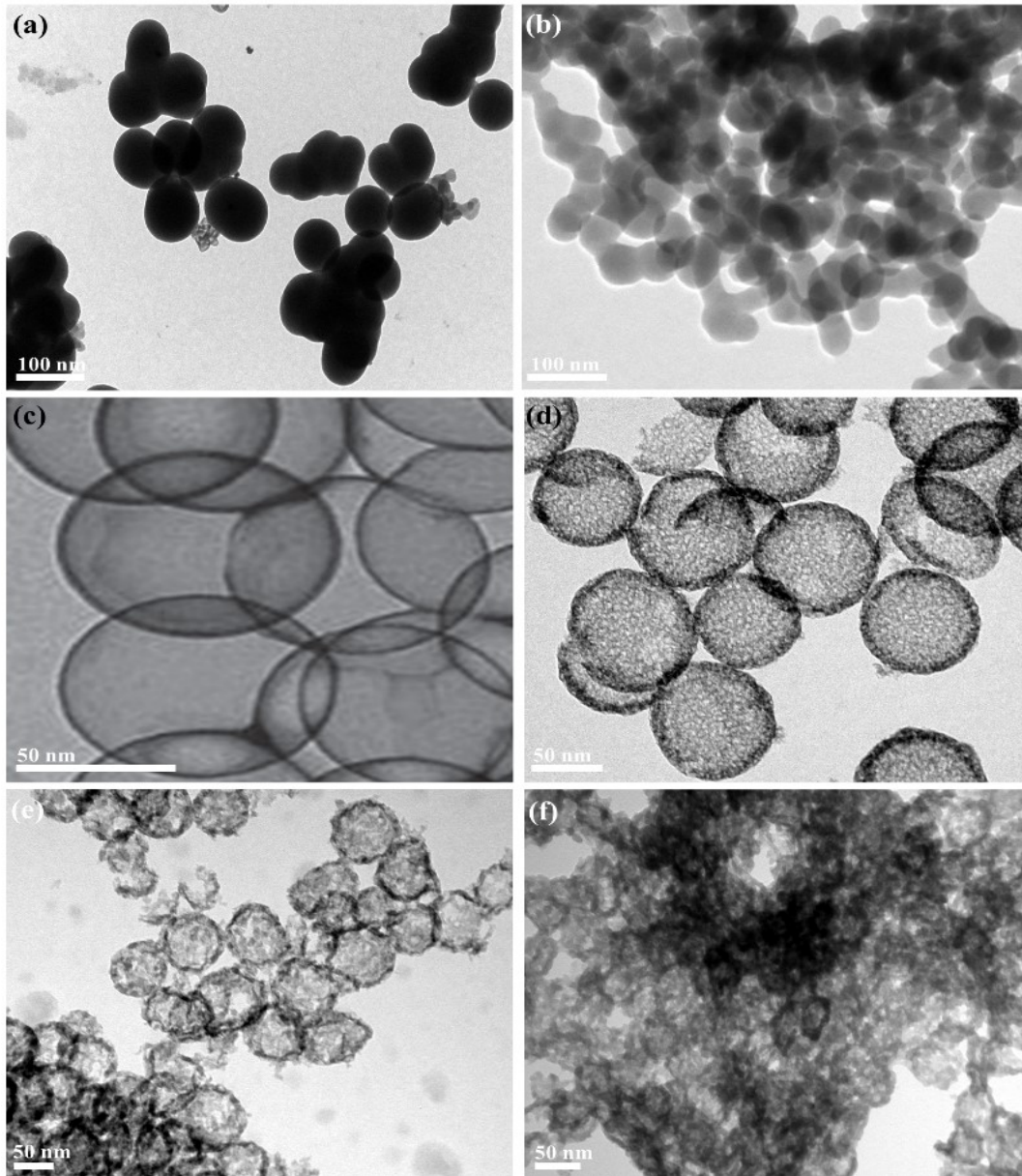
Figure S2 Raman spectra of N-HMPC and HMPC.

Figure S3 (a) TEM image of N-HMPC synthesized by addition of TEOS first before NH$_4$OH, (b) quick addition of reagents, (c) in the absence of Pluronic F127, (d) using 0.2 g of Pluronic F127, (e)using 0.05 g of Pluronic F127, and (f) etching SiO$_2$ in KOH (15 Wt. %).
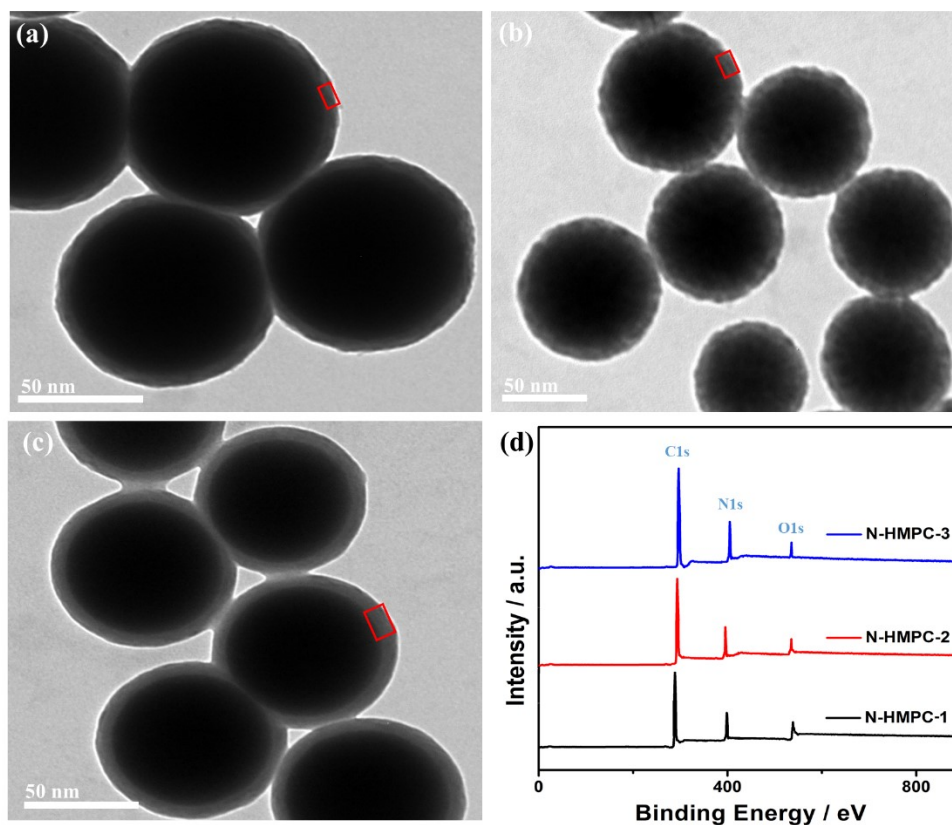
Figure S4 TEM image of (a) N-HMPC-1 obtained using 0.04 g melamine, (b) N-HMPC-2 using 0.09 g melamine, and (c) N-HMPC-3 prepared using 0.13 g melamine. (d) Their XPS surveys. N-HMPC-2 and N-HMPC-1 were synthesized by the same method of N-HMPC-3 but with changing the concertation of melamine.
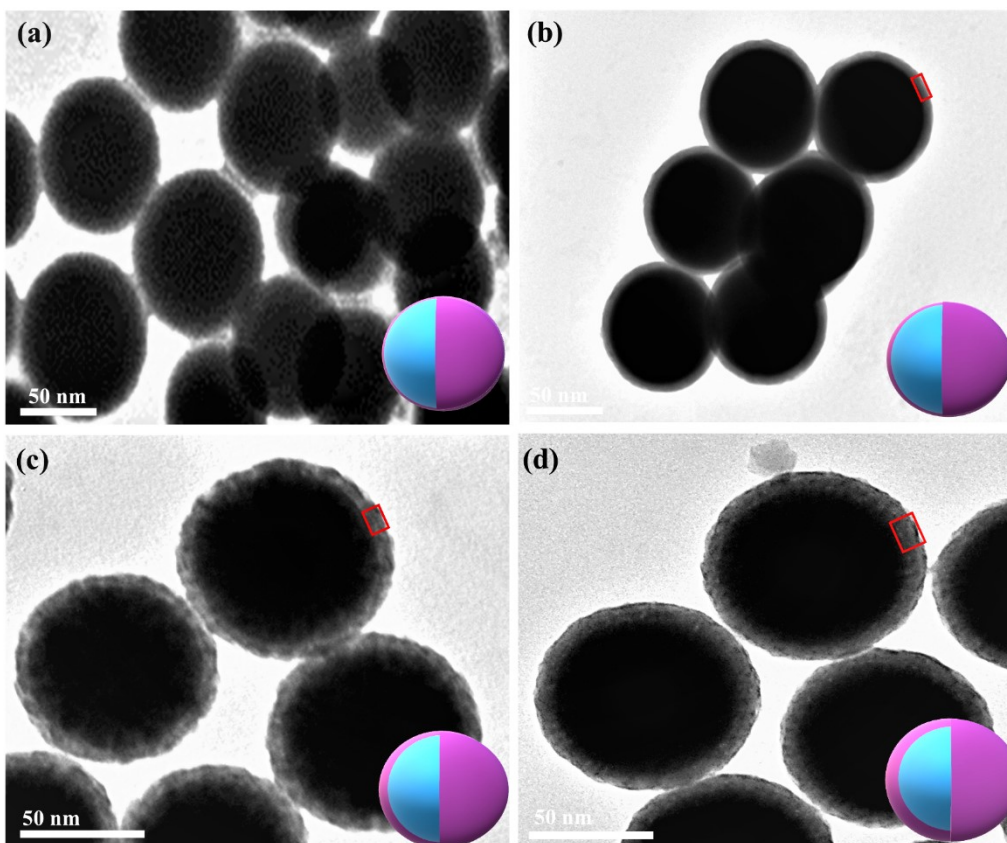
Figure S5 Time-dependent TEM images of N-HMPC growth withdrawn at (a) 1 h, (b), 1.5 min, (c) 3 h, and (d) 5 h of addition of melamine and formaldehyde. The insets in a-d show the 3D models for the difference in the shell thickness.
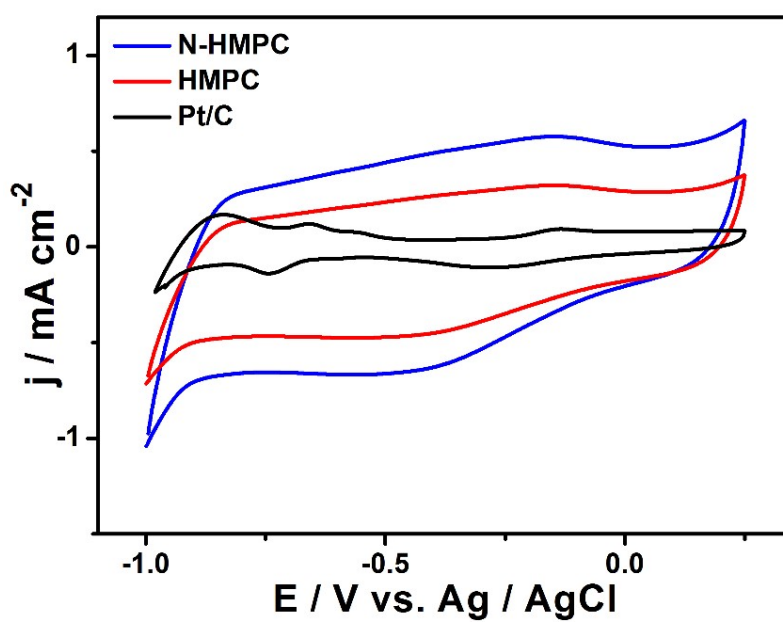

Figure S6 CVs of different catalyst measured in N_2 saturated 0.1 M KOH at a scan rate of 50 m Vs^{-1} at room temperature.
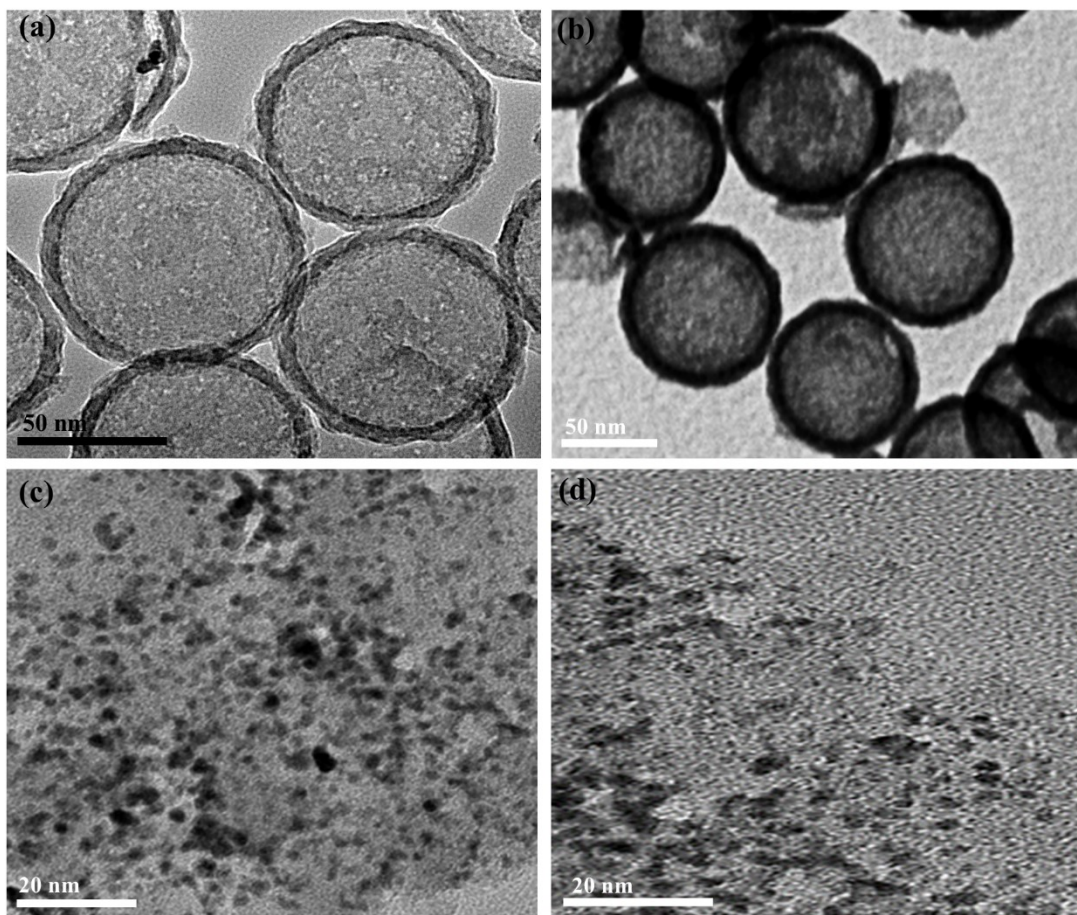
Figure S7 (a-b) TEM images of N-HMPC and (c-d) commercial Pt/C catalyst before and after ORR durability test.

References:

1.   R. Ma, G. Lin, Y. Zhou, Q. Liu, T. Zhang, G. Shan, M. Yang and J. Wang, *NPJ Comput. Mater.,*, 2019, **5**, 1-15.

2.   J. K. Nørskov, F. Abild-Pedersen, F. Studt and T. Bligaard, *Proc. Natl. Acad. Sci.,* 2011, **108**, 937-943.

3.   J. K. Nørskov, J. Rossmeisl, A. Logadottir, L. Lindqvist, J. R. Kitchin, T. Bligaard and H. Jonsson, *J. Phys. Chem. B*, 2004, **108**, 17886-17892.